of norepinephrine production.

Acknowledgments

We thank Dr. Monica Palcic, Chemistry Department, The Ohio State University, for the synthesis and purification of [2-$^2H_2$]dopamine hydrochloride substrate.

Registry No. DM, 51-61-6; [2-$^2H_2$]dopamine hydrochloride, 27160-01-6; (3,4-dimethoxyphenyl)acetonitrile, 93-17-4; 2-(3,4-dimethoxyphenyl)[2-$^2H_2$]ethylamine hydrochloride, 85479-74-9; dopamine β-monooxygenase, 9013-38-1; fumarate, 110-17-8; hydrogen ion, 12408-02-5; deuterium, 7782-39-0.

References

Aunis, D., Miras-Portugal, M. T., & Mandel, P. (1973) *Biochim. Biophys. Acta 327*, 313-327.
Cleland, W. W. (1977) *Adv. Enzymol. Relat. Areas Mol. Biol. 45*, 273-387.
Cleland, W. W. (1979) *Methods Enzymol. 63*, 103-138.
Cook, P. F., & Cleland, W. W. (1981a) *Biochemistry 20*, 1797-1805.
Cook, P. F., & Cleland, W. W. (1981b) *Biochemistry 20*, 1805-1816.
Craine, J. E., Daniels, G. H., & Kaufman, S. (1973) *J. Biol. Chem. 248*, 7838-7844.
Diliberto, E. J., & Allen, P. L. (1981) *J. Biol. Chem. 256*, 3385-3393.
Fersht, A. (1977) *Enzyme Structure and Mechanism*, pp 134-155, W. H. Freeman, San Francisco, CA.
Goldstein, M., Joh, T. H., & Garvey, T. Q., III (1968) *Biochemistry 7*, 2724-2730.
Klinman, J. P., & Krueger, M. (1982) *Biochemistry 21*, 67-75.
Klinman, J. P., Humphries, H., & Voet, J. G. (1980) *J. Biol. Chem. 255*, 11648-11651.
Knowles, J. R. (1976) *CRC Crit. Rev. Biochem. 4*, 165-173.
Kvassman, J., & Pettersson, G. (1978) *Eur. J. Biochem. 87*, 417-427.
Levin, E. Y., Levenberg, B., & Kaufman, S. (1960) *J. Biol. Chem. 235*, 2080-2086.
May, S. W., Phillips, R. S., Mueller, P. W., & Herman, H. H. (1981) *J. Biol. Chem. 256*, 8470-8475.
Miller, S. M., & Klinman, J. P. (1982) *Methods Enzymol. 87*, 711-732.
Miller, S. M., & Klinman, J. P. (1983) *Biochemistry* (preceding paper in this issue).
Miras-Portugal, M. T., Aunis, D., & Mandel, P. (1973) *FEBS Lett. 34*, 140-142.
Njus, D., & Radda, G. K. (1978) *Biochim. Biophys. Acta 463*, 219-244.
Northrop, D. B. (1981) *Biochemistry 20*, 4056-4061.
Rosenberg, R. C., & Lovenberg, W. (1980) *Essays Neurochem. Neuropharmacol. 4*, 163-209.
Skotland, T., & Ljones, T. (1979a) *Inorg. Perspect. Biol. Med. 2*, 151-180.
Skotland, T., & Ljones, T. (1979b) *Eur. J. Biochem. 94*, 145-151.
Skotland, T., & Ljones, T. (1980) *Biochim. Biophys. Acta 630*, 30-35.
Terland, O., & Flatmark, T. (1975) *FEBS Lett. 59*, 52-56.
Vigny, A., & Henry, J. P. (1982) *Biochem. Biophys. Res. Commun. 106*, 1-7.
Villafranca, J. J. (1981) *Met. Ions Biol. 3*, 263-289.
Von Euler, U. S., & Floding, I. (1955) *Acta Physiol. Scand., Suppl. No. 118*, 45-56.

Polypeptide Clearing in Model Membranes: An Analysis of the Partition of Gramicidin A′ between Cadmium Ion Induced Gel and Liquid-Crystalline Phases in Vesicles of Phosphatidic Acid and Phosphatidylcholine†

Gerald W. Feigenson

ABSTRACT: Using a simple model for a biological membrane we examine cation-induced gel phase formation and the depletion of polypeptide from the gel phase. The model system consists of vesicles of phosphatidic acid and phosphatidylcholine which contain gramicidin A′. By use of electron spin resonance to monitor lipid phase behavior, Cd^{2+} is found to induce gel and liquid-crystal phase coexistence over a wide range of lipid composition. Quenching of gramicidin A′ tryptophanyl fluorescence by spin-labeled phosphatidic acid or spin-labeled phosphatidylcholine is analyzed to obtain the partition coefficient, K_p, for gramicidin A′ between gel and liquid-crystal phases. The value of $K_p = 3$ favoring the liquid-crystal phase indicates a partial clearing of the membrane-bound polypeptide from Cd^{2+}-induced gel phase regions of the membrane.

Electron microscopy of fusing biological membranes utilizing fixed and stained thin sections and cryoprotected freeze–fracture has revealed membrane regions in contact to be relatively free of protein (Chi et al., 1979; Lawson et al., 1977; Orci et al., 1977; Peixoto de Menezes & Pinto da Silva, 1978; Kalderon & Gilula, 1979). This finding has been disputed by workers using rapidly frozen membrane samples without cryoprotectant (Chandler & Heuser, 1979, 1980; Ornberg & Reese, 1981). These latter studies suggest that the regions of initial contact of fusing membranes are probably too small in area to allow detection of the putative clearing of intramembrane particles. Freeze–fracture electron microscopy of reconstituted model membranes containing Ca^{2+} ATPase from sarcoplasmic reticulum (Kleemann & McConnell, 1976) or glycophorin (Grant & McConnell, 1974) showed particle-free regions thought to correspond to patches of

† From the Section of Biochemistry, Molecular and Cell Biology, Clark Hall, Cornell University, Ithaca, New York 14853. *Received November 10, 1982.* This work was supported by a grant from the National Institutes of Health, U.S. Public Health Service (HL-18255). This work was done during the tenure of an Established Investigatorship of the American Heart Association.

0006-2960/83/0422-3106$01.50/0

thermotropic gel phase lipid. Portis et al. (1979) have suggested that a rigid complex of Ca^{2+} with acidic phospholipids could form a bilayer region which excludes proteins.

The question of whether multivalent cations cause gel phase formation and consequent clearing of protein from certain regions of a membrane can be posed in precise terms of physical chemistry for a simple model system consisting of a membrane-bound polypeptide and coexisting gel and liquid-crystalline phases: what is the partition coefficient of the polypeptide between the phases?

The problem of measuring such a partition coefficient for coexisting (thermotropic) gel and liquid-crystalline phase phosphatidylcholines was solved in this laboratory by using the quenching of protein intrinsic fluorescence by spin-labeled phosphatidylcholine (London & Feigenson, 1981a). Analysis of fluorescence quenching data to obtain the partition coefficient requires knowing the amounts and the compositions of the coexisting lipid phases.

This paper describes electron spin resonance (ESR)[1] experiments which characterize the lipid phase behavior and fluorescence quenching experiments which are sensitive to polypeptide redistribution caused by cation-induced gel phase formation in model membranes. Phosphatidic acid (PA) is the negatively charged lipid which is examined, based upon our ability to synthesize and to purify the spin-labeled version of PA. Cd^{2+} is the multivalent cation used because of its pronounced effect on PA phase behavior observed in preliminary experiments (Feigenson, 1982). Gramicidin A′, a M_r 1900 membrane-bound polypeptide (Sarges & Witkop, 1964), is readily available commercially and is fluorescent, having four tryptophanyl groups.

Materials and Methods

Egg PC (1,2-diacyl-*sn*-glycero-3-phosphocholine derived from hen egg yolks) and egg PA (lyophilized disodium form) from Avanti were used without further purification. The spin-labeled phospholipids (7,6)PC and (7,6)PA were synthesized as described previously (London & Feigenson, 1981b,c). DPH (diphenylhexatriene) was obtained from Aldrich. Gramicidin A′ ("gramicidin D") and Hepes buffer were from Sigma. $CdCl_2$, anhydrous, was Fisher, A.C.S. grade. All other chemicals were reagent grade.

Samples for fluorescence or ESR measurements were prepared by mixing stock chloroform solutions of PA, PC, and gramicidin A′ or DPH in a 13 × 100 mm Pyrex tube. Chloroform was removed under a stream of nitrogen followed by vacuum pumping for 1 h in the dark. Buffer was added (10 mM Hepes and 100 mM KCl, pH 7.0) to give a total lipid concentration of 0.3 mM for fluorescence measurements or 2 mM for ESR measurements. Samples were sonicated for 1 min under argon in a bath sonicator (Laboratory Supplies Co., Inc.). At this stage, for experiments with Cd^{2+} equilibrated across the vesicles, an aliquot of 200 mM $CdCl_2$ was added to give a final Cd^{2+} concentration of 2 mM (8 mM for ESR). The sample was then frozen in liquid N_2, thawed, and sonicated for 30 s. The freeze–thaw–sonication step was repeated. All samples were prepared in this manner except for the multilamellar vesicle (MLV) samples used to establish light scattering limitations.

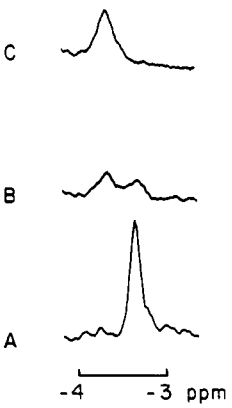

FIGURE 1: ^1H NMR spectra of choline methyl signals to monitor ion permeation across egg PA/egg PC sonicated vesicles. (A) No ion addition. (B) Pr^{3+} added to 2 mM. (C) Sample in (B) frozen in liquid N_2, thawed, and sonicated 30 s. The mole fraction of egg PA in the vesicles is 0.5 and the total lipid 0.5 mM in D_2O. Spectra obtained at 79.54 MHz, 30 °C. 1000 transients were collected with an acquisition time of 0.3 s and a sensitivity enhancement giving 5-Hz line broadening.

Fluorescence measurements were made on a home-built spectrofluorometer [previously described, Caffrey & Feigenson (1981)] with double monochromators in both emission and excitation optics. For samples containing tryptophanyl or DPH, the excitation wavelength was 287 or 360 nm, and the emission wavelength was 340 or 430 nm, respectively. Nominal bandwidths were 4 nm for excitation and 16 nm for emission. Samples for ESR measurements were placed in glass capillary tubes and spectra recorded on a Varian E-3 spectrometer and then entered into the computer (PDP-11/23) by using a graphics tablet. ^1H NMR spectra were obtained at 79.54 MHz on a Varian CFT-20 NMR spectrometer.

Results

Because some of these experiments involve adding ions to lipid vesicles, we determined the conditions required to equilibrate multivalent cations across these vesicles. The permeation was monitored by using the lanthanide-induced shift of PC choline methyl protons [see, for example, Hauser et al. (1975)]. Figure 1A shows a region of the ^1H NMR spectrum of a typical sample, sonicated vesicles of egg PA/egg PC = 0.5/0.5, 0.5 mM total lipid. In Figure 1B 2 mM Pr^{3+} has been added, splitting the choline methyl signal into a shifted peak and an unshifted peak. On the basis of the observed splitting, the vesicle remains impermeable to Pr^{3+} for at least several hours. In order to examine whether the cations could be equilibrated across the vesicle, the sample used in Figure 1B was frozen in liquid N_2, thawed, and then sonicated for 30 s. The single shifted choline methyl peak in Figure 1C shows that the freeze–thaw–sonication procedure creates at least close to equal ion concentrations across the vesicle. Similar lanthanide-induced shift results were obtained with Dy^{3+}, Tm^{3+}, and Eu^{3+} and for vesicles containing egg PC without egg PA.

In the fluorescence quenching experiments described below, the lipid concentration must be low enough that the largest possible light scattering changes have no significant effect on measured fluorescence, e.g., small vesicles changing to large multilamellar vesicles (MLV). Figure 2 shows that the

[1] Abbreviations: ESR, electron spin resonance; ^1H NMR, proton nuclear magnetic resonance; MLV, multilamellar vesicles; SUV, small unilamellar vesicles; Hepes, *N*-(2-hydroxyethyl)piperazine-*N*′-2-ethanesulfonic acid; DPH, 1,6-diphenyl-1,3,5-hexatriene; PA, 1,2-diacyl-*sn*-glycero-3-phosphoric acid; PC, 1,2-diacyl-*sn*-glycero-3-phosphocholine; (7,6)PA, 1-acyl-2-[2-(6-carboxyhexyl)-2-octyl-4,4-dimethyloxazolidinyl-3-oxy]-*sn*-glycero-3-phosphoric acid; (7,6)PC, 1-acyl-2-[2-(6-carboxyhexyl)-2-octyl-4,4-dimethyloxazolidinyl-3-oxy]-*sn*-gylcero-3-phosphocholine; DMPC, 1,2-dimyristoyl-*sn*-glycero-3-phosphocholine; DSPC, 1,2-distearoyl-*sn*-glycero-3-phosphocholine; DPPC, 1,2-dipalmitoyl-*sn*-glycero-3-phosphocholine; PS, 1,2-diacyl-*sn*-glycero-3-phosphoserine; ATPase, adenosinetriphosphatase; EDTA, ethylenediaminetetraacetic acid; G, gauss.

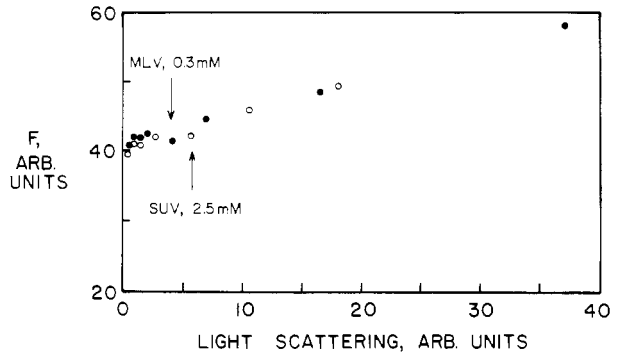

FIGURE 2: Measured fluorescence of 2×10^{-5} M tryptophan as a function of sample turbidity. (○) In the presence of small unilamellar vesicles (SUV); (●) in the presence of multilamellar vesicles (MLV). 10 mM SUV sonicated to clarity or 10 mM MLV as a coarse, vortexed dispersion were diluted and then added to a tryptophan solution, all in 10 mM Hepes and 100 mM KCl, pH 7.0. Fluorescence was measured (arbitrary units) with λ_{ex} = 287 nm and λ_{em} = 340 nm. The turbidity was monitored by 90° light scattering measured with $\lambda_{ex} = \lambda_{em}$ = 340 nm.

fluorescence observed for a dilute tryptophan solution is increased less than 5% by the addition of small unilamellar vesicles up to 2.5 mM or MLV up to 0.3–0.4 mM. [We note that in our experiments the detected fluorescence has a negligible contribution from Rayleigh, Tyndall, or Raman scattering, and therefore Figure 2 shows an authentic increase in measured fluorescence caused by light scattering (Kuntz et al., 1966).] Finally, in order to verify that at this lipid concentration scattering does not affect the measured fluorescence, tryptophan fluorescence was determined in buffer or in 0.3 mM lipid vesicles of egg PA/egg PC with 2 mM Cd^{2+} equilibrated by freeze–thaw–sonication. The measured fluorescence is unaffected by vesicles of any PA mole fraction. All fluorescence data in the following experiments were therefore obtained at an overall lipid concentration of 0.3 mM.

The study of the effect of Cd^{2+} upon the local lipid environment of gramicidin A′ begins with an experiment which is sensitive to the contact of spin-labeled phospholipid with membrane-bound fluorophors. The quenching of gramicidin A′ tryptophanyl fluorescence as a function of spin-labeled phospholipid concentration in the vesicles is shown in Figure 3. Since the (7,6)PA/egg PC fluorescence quenching curve is so similar to the (7,6)PC/egg PC curve, the local lipid environment of the tryptophanyl residues is not selectively enriched in either PA or PC.

When 2 mM Cd^{2+} is added and equilibrated across the vesicles, the gramicidin A′ fluorescence markedly increases in (7,6)PA/egg PC but not in (7,6)PC/egg PC. This fluorescence enhancement, or relief of quenching, might be described by a weaker binding of a (7,6)PA–Cd^{2+} complex to the gramicidin A′. However, if the cation induces a phase separation, then the system is more properly described by the lipid phase characteristics together with the partition coefficient of gramicidin A′ between the phases.

Although the cation-sensitive phase behavior of phospholipids can be characterized rather directly by X-ray diffraction, as we have done for egg PA/egg PC (unpublished experiments), we lack sufficient (7,6)PA for such experiments. Instead, we utilize the sensitivity of ESR to both the concentration and the mobility of spins in order to determine phase composition and phase type (liquid crystal or gel). The ESR spectra of vesicles of several different (7,6)PA/egg PC ratios are shown in Figure 4A. The line width increases as the spin concentration increases because of spin exchange and dipole–dipole interactions (Scandella et al., 1972). [Note that

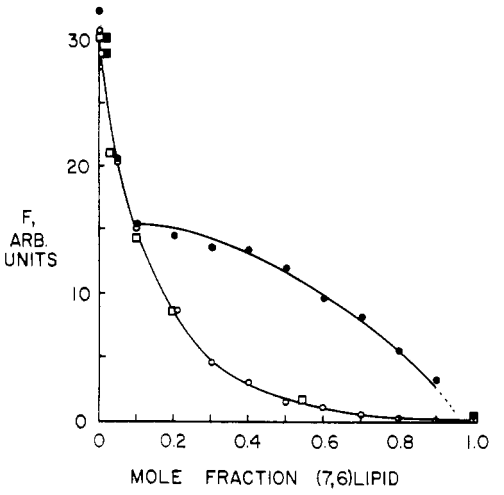

FIGURE 3: Fluorescence quenching of gramicidin A′ tryptophanyl in model membranes containing spin-labeled lipid. The abscissa is the mole fraction of spin-labeled lipid in the membrane. (7,6)PA/egg PC with (●) or without (○) 2 mM Cd^{2+}; (7,6)PC/egg PC with (■) or without (□) 2 mM Cd^{2+}. Total lipid concentration in 0.3 mM. Mole ratio of gramicidin to lipid is 1/200.

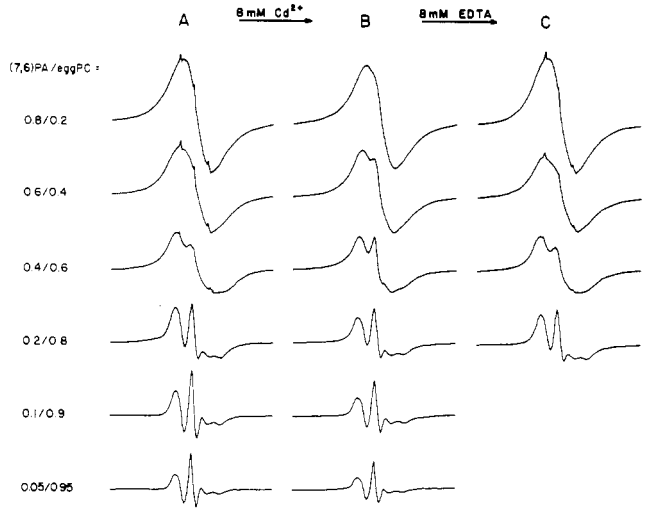

FIGURE 4: ESR spectral dependence on (7,6)PA concentration and on addition or chelation of Cd^{2+}. 2 mM freeze–thaw–sonicated vesicles of varying mole ratios of (7,6)PA/egg PC were observed (A) in 10 mM Hepes and 100 mM KCl, pH 7.0. (B) With Cd^{2+}, pH 7, added to 8 mM to the samples in (A) followed by two cycles of freeze–thaw–sonication. (C) With EDTA, pH 7, added to 8 mM to the samples in (B) followed by two cycles of freeze–thaw–sonication.

the sharp three-line spectra observed at [(7,6)PA] > 0.4 arise from an aqueous impurity, probably the (7,6) fatty acid, which comprises <0.1% of the integrated ESR signal.] The spectra in Figure 4B are obtained by adding Cd^{2+} to 8 mM, followed by two cycles of freeze–thaw–sonication. This Cd^{2+} addition has little apparent effect for [(7,6)PA] = 0.05 or 0.10. However, for [(7,6)PA] = 0.20, 0.40, or 0.60, the Cd^{2+} gives rise to a sharper spectral component. These spectra which contain both broad and sharp features arise from samples which contain both concentrated (7,6)PA and dilute (7,6)PA phases. When 8 mM EDTA is added to the Cd^{2+}-containing samples, followed by freeze–thaw–sonication, any sharp spectral components produced by Cd^{2+} disappear, as shown in Figure 4C.

Because the spin concentrations are so great in the above experiments, spectral line widths are so broad that we cannot determine whether one of the (7,6)PA-containing phases is a rigid phase. ESR experiments using more dilute (7,6)PA

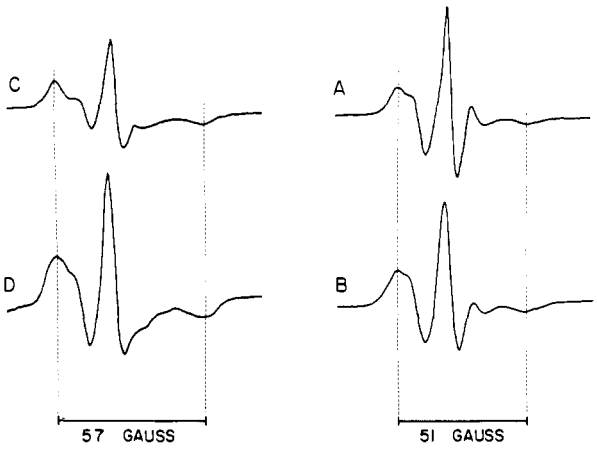

FIGURE 5: ESR spectra of dilute (7,6)PA in gel or in liquid-crystalline model membranes. (A) 80 mM MLV of (7,6)PA/DMPC = 0.005/0.995 at 30 °C. (B) 2 mM freeze–thaw–sonication vesicles of (7,6)PA/egg PA/egg PC = 0.02/0.68/0.30 at 20 °C. (C) 80 mM MLV of (7,6)PA/DSPC = 0.005/0.995 at 30 °C. (D) Sample (B) with Cd^{2+} added to 4 mM followed by two cycles of freeze–thaw–sonication.

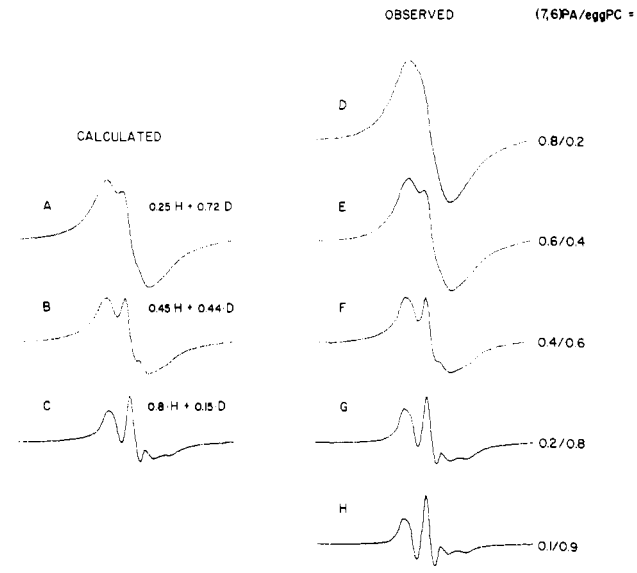

FIGURE 6: ESR spectra of (7,6)PA/egg PC observed in the presence of Cd^{2+} or else calculated as the sum of two observed spectra. (D–H) are traced and digitized from Figure 4B. (A–C) are calculated as a sum of contributions from (H) and (D). The sums are constrained so that the total spectral intensity corresponds to 2 mM total lipid with (7,6)PA/egg PC = 0.6/0.4 (A), 0.4/0.6 (B), or 0.2/0.8 (C).

are shown in Figure 5. For (7,6)PA/DSPC = 0.005/0.995 at 20 °C (Figure 5C), the outer line separation is 57 G for this rigid, gel phase (Ladbrooke & Chapman, 1969). For (7,6)PA/DMPC = 0.005/0.995 at 30 °C (Figure 5A) the outer line separation is 51 G for this liquid-crystalline system (Ladbrooke & Chapman, 1969). As shown in Figure 5B,D, for (7,6)PA/egg PA/egg PC = 0.02/0.68/0.30, the outer line separation of about 51 G observed in the absence of Cd^{2+} increases to 57 G in the presence of Cd^{2+}.

The ESR experiments (Figures 4 and 5) confirm that vesicles of (7,6)PA/egg PC ± Cd^{2+} have phase behavior similar to that of the unlabeled lipids as determined by X-ray diffraction. In order to test whether Cd^{2+} causes the separation of two phases each of well-defined composition, the ESR spectra of Figure 4B can be simulated as the sum of two spectra (Figure 6). The spectra from Figure 4B were digitized and those for [(7,6)PA] = 0.10 and 0.80 were added in varying ratios, with the constraint that total spectral intensity corresponded to [(7,6)PA] = 0.20, 0.40, or 0.60. Figure 6 shows that spectra can be calculated in this way to provide a good match with the spectra observed. Note that the dilute (7,6)PA phase and the concentrated (7,6)PA phase which actually coexist do not necessarily have exactly the same compositions as those of the spectra used in these simulations. However, the compositions of the phase boundaries can be calculated from the simulations shown in Figure 6: the ratio of the moles of (7,6)PA in the gel phase to the moles of (7,6)PA in the liquid-crystalline phase is

$$\frac{(7,6)PA_G}{(7,6)PA_{LC}} = \frac{[(7,6)PA]_G}{[(7,6)PA]_{LC}} \frac{[G]}{[LC]} \quad (1)$$

where [G]/[LC] = the mole ratio of lipids in the gel phase to lipids in the liquid-crystalline phase and $[(7,6)PA]_{G(LC)}$ = at the boundary of the 2-phase region the mole fraction of gel (liquid-crystal) phase which is composed of (7,6)PA. From the lever rule for phase diagrams (Moore, 1962)

$$\frac{[G]}{[LC]} = \frac{[(7,6)PA] - [(7,6)PA]_{LC}}{[(7,6)PA]_G - [(7,6)PA]} \quad (2)$$

where [(7,6)PA] = overall mole fraction of (7,6)PA in the vesicles. Combining eq 1 and 2 gives

$$\frac{(7,6)PA_G}{(7,6)PA_{LC}} = \frac{[(7,6)PA]_G}{[(7,6)PA]_{LC}} \frac{[(7,6)PA] - [(7,6)PA]_{LC}}{[(7,6)PA]_G - [(7,6)PA]} \quad (3)$$

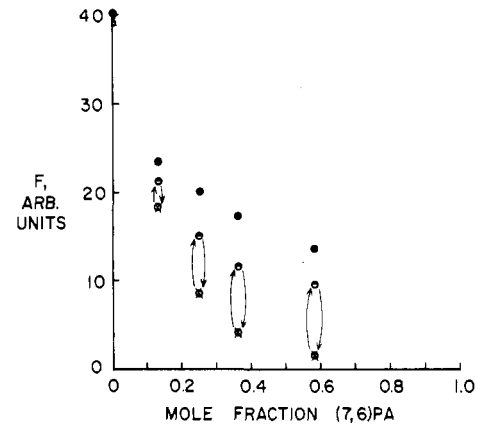

FIGURE 7: Fluorescence quenching of gramicidin A′ in (7,6)PA/egg PC vesicles. (○) No additions to the buffer; (⊖) Cd^{2+} added to 2 mM outside the vesicles; (×) 2.5 mM EDTA added to the vesicles with 2 mM Cd^{2+} outside; (●) 2 mM Cd^{2+} equilibrated across vesicles. The ratio of gramicidin to lipid is 1/200.

The ratio in eq 3 is found from the simulations shown in Figure 6. The value of [(7,6)PA] is known for each sample preparation. This leaves eq 3 having as the two unknowns the (7,6)PA concentrations at the phase boundaries. Solving for these two concentrations using linear regression for the data in Figure 6A–C, we calculate that at 20 °C the liquidus line is at $[(7,6)PA]_{LC}$ = 0.09 ± 0.01 and the solidus line at $[(7,6)PA]_G$ = 0.80 ± 0.10.

The ESR experiment shown in Figure 4C suggests that the gel–liquid-crystalline phase separation is reversible. We tested whether the fluorescence quenching experiments would likewise show reversibility upon Cd^{2+} chelation. Cd^{2+} (final concentration 2 mM) was added to vesicles containing gramicidin A′ in (7,6)PA/egg PC (Figure 7). After the fluorescence was measured in the presence of the external 2 mM Cd^{2+}, 2.5 mM EDTA was added to the sample. Figure 7 shows that EDTA exactly reverses the Cd^{2+} fluorescence enhancements. Also shown in this figure are fluorescence measurements for samples sonicated initially in the presence of 2 mM Cd^{2+} followed by two cycles of freeze–thaw–sonication. These measurements

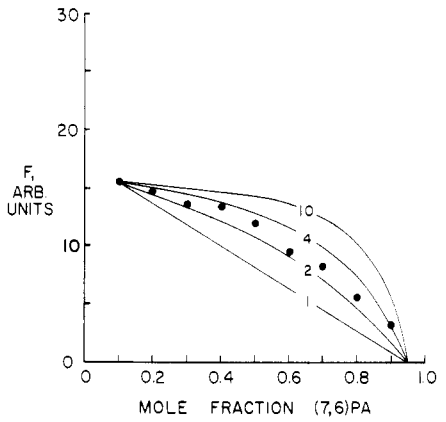

FIGURE 8: Fitting gramicidin A′ fluorescence quenching observed in the presence of Cd^{2+} to fluorescence quenching calculated for gramicidin partition between gel and liquid-crystalline phases. (●) Fluorescence observed (Figure 3). Curves are calculated by using eq 4 (text) for the indicated values of the partition coefficient for gramicidin between a rigid phase of (7,6)PA mole fraction 0.95 and a liquid-crystalline phase of (7,6)PA mole fraction 0.10.

show that the relief of fluorescence quenching by Cd^{2+} is significantly greater when Cd^{2+} is present on both sides of the vesicles compared to only the outside of the vesicles.

The fluorescence quenching behavior of gramicidin A′ in (7,6)PA/egg PC (Figure 3) can be analyzed to obtain the partition coefficient, K_p, of gramicidin A′ between gel and liquid-crystalline phases. I use the analysis developed by London & Feigenson (1981a) to write

$$F = (F)_{LC} + \frac{[G]}{K_p(1 - [G]) + [G]}[(F)_G - (F)_{LC}] \quad (4)$$

where F = measured or calculated fluorescence intensity, $(F)_{G\text{ or }LC}$ = fluorescence in a membrane of the composition at the gel (or liquid-crystalline) phase boundary, and

$$[G] = \frac{[(7,6)PA]_{LC} - [(7,6)PA]}{[(7,6)PA]_{LC} - [(7,6)PA]_G}$$

Figure 8 shows that the data of Figure 3 are well fit by using $K_p = 3$ (partition in favor of the PC-rich liquid-crystalline phase) with $[(7,6)PA]_{LC} = 0.10$ and $[(7,6)PA]_G = 0.95$.

In order to test this method of finding K_p, a similar system was examined in which the spin-label is switched from PA to PC. If the phase behavior of egg PA/(7,6)PC in the presence of Cd^{2+} is similar to that of (7,6)PA/egg PC, then an analysis of gramicidin fluorescence quenching should yield a similar partition coefficient. One difficulty arises in this experiment, that for egg PA/(7,6)PC > 0.8, especially in the presence of Cd^{2+}, sample precipitation gives rise to unreliable data. Nonetheless, it is necessary to know the fluorescence in the absence of spin-labeled lipid in order to analyze the fluorescence quenching. This fluorescence was obtained by preparing vesicles containing gramicidin A′ in different mixtures of egg PA/egg PC ± Cd^{2+} and then extrapolating to egg PA/egg PC = 1/0. Figure 9 shows the fluorescence quenching data for egg PA/(7,6)PC. Also shown are calculated curves (eq 4) for several values of K_p (again, $K_p > 1$ indicates partition in favor of the liquid-crystalline phase). Although the fit is not impressive, $K_p = 3$ best describes the data.

For comparison with this partition coefficient of $K_p = 3$ for gramicidin A′, the fluorescence quenching of DPH in (7,6)-PA/egg PC was measured in the presence and absence of 2 mM Cd^{2+} (Figure 10). In the presence of Cd^{2+} the fluorescence is linear as a function of the (7,6)PA concentration. This linearity is fit precisely by $K_p = 1$. Note that this straight line intersects the quenching curve obtained in the absence of Cd^{2+} at (7,6)PA concentrations of 0.08 and 0.95, in good agreement with Figure 3 and with the ESR spectral simulations.

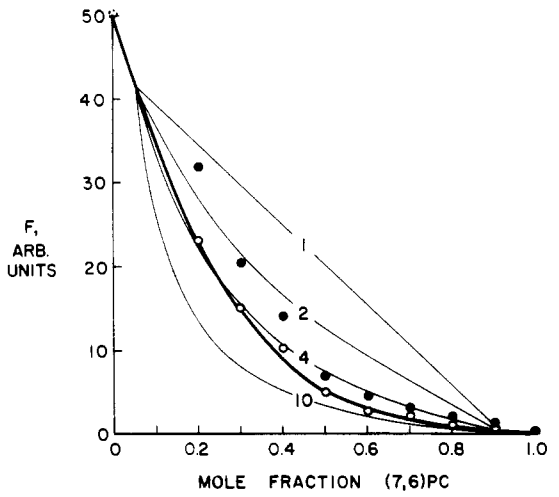

FIGURE 9: Calculated and observed fluorescence quenching of gramicidin A′ in egg PA/(7,6)PC vesicles. (○) Without Cd^{2+}; (●) in the presence of 2 mM Cd^{2+}; (broken circle) extrapolated from egg PA/egg PC ± 2 mM Cd^{2+} as [egg PC] → 0. A heavy line is drawn through the data points for fluorescence without Cd^{2+}. Curves are calculated by using eq 4 (text) for the indicated values of the partition coefficient for gramicidin between a rigid phase of egg PA mole fraction 0.95 and a liquid-crystalline phase of egg PA mole fraction 0.10. The ratio of gramicidin to lipid is 1/200.

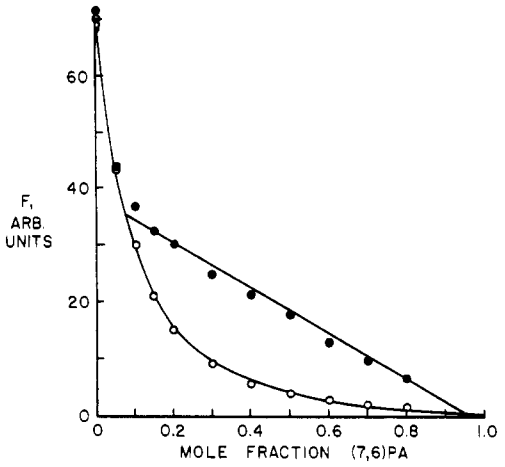

FIGURE 10: Fluorescence quenching of DPH in (7,6)PA/egg PC vesicles. (○) Without Cd^{2+}; (●) in the presence of 2 mM Cd^{2+}. The ratio of DPH to lipid is 1/200.

Discussion

In the experiments described here we consider how a membrane-bound polypeptide responds when a multivalent cation induces a gel phase to form. For gramicidin A′ we find a value of the partition coefficient, $K_p = 3$, favoring the liquid-crystalline phase. This value gains reliability in being found for two different PA/PC systems: one with the spin-label on the PA and the other with the spin-label on the PC. The value of 3 is sufficiently greater than unity as to indicate a partial clearing of polypeptide out of the gel phase. In this way we establish a molecular-level basis for the electron microscopy observations that protein is cleared from fusing regions of membranes (Chi et al., 1976; Lawson et al., 1977; Orci et al., 1977; Peixoto de Menezes & Pinto da Silva, 1978; Kalderon & Gilula, 1979). Still, this value is much less than

the value K_p = 100, describing preferential partitioning of gramicidin A′ into a liquid-crystalline egg PC phase from a thermotropic gel phase of DPPC (London & Feigenson, 1981a). It could be that the PA–Cd^{2+} gel phase is more disordered than is the DPPC gel phase and thereby accommodates the gramicidin A′. If so, then other negatively charged phospholipids and other cations could form gels with widely different polypeptide-solubilizing properties. Furthermore, we expect that the partition coefficient could be a strong function of polypeptide size, if solubility in the gel phase involves accommodation to defects in lipid packing.

The analysis of fluorescence quenching data to obtain a partition coefficient requires knowing the compositions and the amounts of the phases, i.e., the phase diagram. We have determined partial phase diagrams for egg PA with egg PC, DMPC, and DPPC, with and without Cd^{2+} using X-ray diffraction (unpublished experiments). In the present study, insufficient (7,6)PA was available to construct a phase diagram in this way. However, the ESR experiments (Figures 4 and 5) clearly show that Cd^{2+} induces a PA-rich gel phase to form in coexistence with a PC-rich liquid-crystalline phase. The compositions of the phases virtually can be read from the fluorescence quenching curves of Figures 3 and 10: the curve of fluorescence in the presence of Cd^{2+} intersects the curve for fluorescence in the absence of Cd^{2+} at approximately [(7,6)PA] = 0.09 and 0.95. These two compositions mark the boundaries of the two-phase region. In comparison the analysis of the ESR data shown in Figure 6 (see Results) yields phase boundaries at [(7,6)PA] = 0.09 ± 0.01 and 0.80 ± 0.10. These concentrations are in reasonable agreement with the fluorescence results.

Using the same methodology by which we obtain K_p = 3 for gramicidin A′, we obtain K_p = 1 for DPH partition between Cd^{2+}-induced gel and liquid-crystalline phases of (7,6)PA/egg PC. This is the same value for K_p found previously for DPH partition between (thermotropic) gel and liquid-crystalline phases of either DPPC and DMPC (Lentz et al., 1976) or DPPC/(7,6)PC (London & Feigenson, 1981a).

Ito & Ohnishi (1974) have previously used ESR to show that several multivalent cations induce the coexistence of two phases for PA/PC multilayers bound to a filter support. These investigators have also determined a partial phase diagram for PS/PC multilayers in the presence of Ca^{2+} (Tokutomi et al., 1981).

Cd^{2+} was used in the studies reported here because it has the largest effects on fluorescence quenching behavior in (7,6)PA/egg PC of a number of divalent cations (Feigenson, 1982). Although Cd^{2+} is sometimes said to be a Ca^{2+} analogue (same charge and almost the same ionic radius), Cd^{2+} is much more electropositive than Ca^{2+} and forms tighter complexes (Chaberek & Martell, 1959). Thus, extrapolation of Cd^{2+} effects to embrace other multivalent cations should be done with caution.

Figures 4 and 7 show that the Cd^{2+}-induced gel phase formation and consequent gramicidin redistribution are reversible by EDTA. The experiments depicted in Figure 7 show reversibility to be complete in less than about 10 s, which is the time required to mix the sample and then to measure the fluorescence. These results suggest, but do not prove, that the phase separation is lateral, in the plane of the membrane, as opposed to a bulk separation of a PA–Cd^{2+}-rich gel phase (Van Dijck et al., 1978).

This work establishes that multivalent cations can induce a negatively charged phospholipid to form a gel phase which is *relatively* cleared of membrane-bound polypeptide. Such protein clearing *might* be part of a mechanism for membrane fusion. However, an important aspect of such a step is not yet determined: does the formation of gel and/or protein clearing require that two bilayers be closely apposed? [Note the distinction made by Papahadjopoulos and co-workers between cis and trans cation–PS complexes (Portis et al., 1979).] Liao & Prestegard (1981) have suggested that Cd^{2+} can bridge the head groups between bilayers of multilamellar PA. In the present study we have not established whether protein clearing can be observed when vesicles are unequivocally unilamellar or whether multilayers are required. These determinations are now under way.

Acknowledgments

I gratefully acknowledge helpful discussions with Paul Meers, Martin Caffrey, Bob Bayer, Erwin London, and Barbara Baird. Bob Bayer wrote the computer programs. Monique Sessler synthesized the (7,6)PA.

Registry No. Gramicidin A′, 9066-06-2; cadmium, 7440-43-9.

References

Caffrey, M., & Feigenson, G. W. (1981) *Biochemistry 20*, 1949–1961.

Chaberek, S., & Martell, A. E. (1959) in *Organic Sequestering Agents*, pp 166, 572, Wiley, New York.

Chandler, D. E., & Heuser, J. (1979) *J. Cell Biol. 83*, 91–108.

Chandler, D. E., & Heuser, J. E. (1980) *J. Cell Biol. 86*, 666–674.

Chi, E. Y., Lagunoff, D., & Koehler, J. K. (1976) *Proc. Natl. Acad. Sci. U.S.A. 73*, 2823–2827.

Feigenson, G. W. (1982) *Biophys. J. 37*, 165.

Grant, C. W. M., & McConnell, H. M. (1974) *Proc. Natl. Acad. Sci. U.S.A. 71*, 4653–4657.

Hauser, H., Phillips, M. C., Levine, B. A., & Williams, R. J. P. (1975) *Eur. J. Biochem. 58*, 133–144.

Ito, T., & Ohnishi, S. (1974) *Biochim. Biophys. Acta 352*, 29–37.

Kalderon, N., & Gilula, N. B. (1979) *J. Cell Biol. 81*, 411–425.

Kleemann, W., & McConnell, H. M. (1976) *Biochim. Biophys. Acta 419*, 206–222.

Kuntz, E., Bishai, F., & Augenstein, L. (1966) *Nature (London) 212*, 980–983.

Ladbrooke, B. D., & Chapman, D. (1969) *Chem. Phys. Lipids 3*, 304–356.

Lawson, D., Raff, M. C., Gomperts, B., Fewtrell, C., & Gilula, N. B. (1977) *J. Cell Biol. 72*, 242–259.

Lentz, B. R., Barenholz, Y., & Thompson, T. E. (1976) *Biochemistry 15*, 4529–4537.

Liao, M. J., & Prestegard, J. H. (1981) *Biochim. Biophys. Acta 645*, 149–156.

London, E., & Feigenson, G. W. (1981a) *Biochim. Biophys. Acta 649*, 89–97.

London, E., & Feigenson, G. W. (1981b) *Biochemistry 20*, 1932–1938.

London, E., & Feigenson, G. W. (1981c) *Biochemistry 20*, 1939–1948.

Moore, W. J. (1962) in *Physical Chemistry*, 3rd ed., p 128, Prentice-Hall, Englewood Cliffs, NJ.

Orci, L., Perrelet, A., & Friend, D. S. (1977) *J. Cell Biol. 75*, 23–30.

Ornberg, R. L., & Reese, T. S. (1981) *J. Cell Biol. 90*, 40–54.

Peixoto de Menezes, A., & Pinto da Silva, P. (1978) *J. Cell Biol. 76*, 767–778.

Portis, A., Newton, C., Pangborn, W., & Papahadjopoulos,

D. (1979) *Biochemistry 18*, 780-789.
Sarges, R., & Witkop, B. (1964) *J. Am. Chem. Soc. 86*, 1862-1863.
Scandella, C. J., Devaux, P., & McConnell, H. M. (1972) *Proc. Natl. Acad. Sci. U.S.A. 69*, 2056-2060.
Tokutomi, S., Lew, R., & Ohnishi, S. (1981) *Biochim. Biophys. Acta 643*, 276-282.
Van Dijck, P. W. M., De Kruijff, B., Verkleij, A. J., Van Deenen, L. L. M., & De Gier, J. (1978) *Biochim. Biophys. Acta 512*, 84-96.

Multiple Sites of Action for Noncompetitive Blockers on Acetylcholine Receptor Rich Membrane Fragments from *Torpedo marmorata*†

Thierry Heidmann, Robert E. Oswald, and Jean-Pierre Changeux*

ABSTRACT: A vast series of compounds, different from the typical nicotinic antagonists, block in a noncompetitive manner the permeability response of several cholinergic synapses (electromotor synapse, neuromuscular junction) to acetylcholine. The interaction of several of these noncompetitive blockers was investigated in vitro with membrane fragments rich in acetylcholine receptor prepared from *Torpedo marmorata* electric organ. First, their effect on the conformational transitions of the membrane-bound receptor was monitored with a fluorescent cholinergic agonist and a rapid-mixing technique. All the compounds tested stabilized to various extents a "desensitized" state of the receptor exhibiting a high affinity for the agonist with minimal effect but with a high affinity in the case of the frog toxin perhydrohistrionicotoxin (H_{12}HTX). H_{12}HTX was then used to distinguish between two categories of effects of the noncompetitive blockers: (1) with some of them (phencyclidine, meproadifen, Triton X-100), the stabilization of the high-affinity state was blocked by H_{12}HTX; (2) with others (chlorpromazine, trimethisoquin), the shift of the conformational equilibrium was insensitive to H_{12}HTX. In the first instance, the stabilization of the high-affinity state took place without noticeable cooperative effects, while in the second, significant positive cooperativity was systematically observed. In a second series of experiments, binding studies were carried out under equilibrium conditions with tritiated derivatives of H_{12}HTX, phencyclidine, meproadifen, Triton X-100, chlorpromazine, and trimethisoquin. All these tritiated ligands bound to "allosteric" sites distinct from the acetylcholine receptor site, but they also bound to some extent to the receptor site. Two main categories of allosteric sites for noncompetitive blockers were distinguished: (1) a "high-affinity" site which was present in one copy per acetylcholine receptor light form (250000 daltons) and blocked by H_{12}HTX and (2) a population of "low-affinity" sites present in large numbers (10-30 sites per molecule of receptor) and insensitive to H_{12}HTX. Comparison of the conformational and binding data led to the conclusion that the high-affinity site was responsible for the H_{12}HTX-sensitive effect of noncompetitive blockers on the conformational transition while the low-affinity sites were engaged in the H_{12}HTX-insensitive ones. In the cases of chlorpromazine and trimethisoquin, low-affinity H_{12}HTX-insensitive binding was significant at concentrations at which the effects on conformational transitions occurred. Reconstitution experiments indicated that the number of these low-affinity sites depended on the lipid to protein ratio, suggesting that these sites are located at the interface of the receptor protein with membrane lipids. It was also shown that the unique high-affinity site for noncompetitive blockers is in contact with all four types of subunits of the receptor molecule. The possibility is considered that this site lies within the central depression of the molecule which potentially may serve as an ion channel.

At the neuromuscular junction and the electromotor synapse, the permeability response of the postsynaptic membrane to the neurotransmitter acetylcholine (AcCh)[1] is blocked by two series of pharmacological agents: the competitive antagonists like *d*-tubocurarine or flaxedil and a heterogeneous group of compounds referred to as noncompetitive blockers (NCBs) [review in Changeux (1981)]. This class of effectors includes aminated local anesthetics such as procaine, lidocaine, dibucaine, proadifen, or dimethisoquin [see Weber & Changeux (1974), Cohen et al. (1974), Weiland et al. (1977), Heidmann & Changeux (1979), Krodel et al. (1979), and Sine & Taylor (1982)], sedatives such as chlorpromazine (Koblin & Lester, 1979), antimalarial drugs such as quinacrine (Grünhagen & Changeux, 1976; Adams & Feltz, 1980), hallucinogens such as phencyclidine (Kloog et al., 1980; Albuquerque et al., 1980; Karpen et al., 1982; Oswald & Changeux, 1981a,b), a frog toxin, histrionicotoxin (Daly et al., 1971; Elliott & Raftery, 1977; Eldefrawi et al., 1980b; Spivak et al., 1982), the lipophilic cation triphenylmethylphosphonium (Lauffer & Hucho, 1982), and a number of

† From the Neurobiologie Moléculaire et Laboratoire Associé au Centre National de la Recherche Scientifique, Interactions Moléculaires et Cellulaires, Institut Pasteur, 75724 Paris Cedex 15, France (T.H., R.E.O., and J.-P.C.), and the Department of Pharmacology, New York State College of Veterinary Medicine, Cornell University, Ithaca, New York 14853 (R.E.O.). *Received November 15, 1982; revised manuscript received March 3, 1983.* This work was supported by grants from the Muscular Dystrophy Association of America, the Fondation Fyssen, the Fondation de France, the Collège de France, the Ministère de la Recherche et de l'Industrie, the Centre National de la Recherche Scientifique, the Institut National de la Santé et de la Recherche Médicale, and the Commissariat à l'Energie Atomique.

[1] Abbreviations: AcCh, acetylcholine; AcChR, acetylcholine receptor; H_{12}HTX, perhydrohistrionicotoxin; Dns-C_6-Cho, 6-[5-(dimethylamino)-1-naphthalenesulfonamido]hexanoic acid β-(methobromide) ethyl ester; NCB, noncompetitive blocker; 5A[^{3}H]T, 5-azido[^{3}H]trimethisoquin; $C_{12}E_8$, octaoxyethylene glycol dodecyl monoether; Tris-HCl, tris(hydroxymethyl)aminomethane hydrochloride; EDTA, ethylenediaminetetraacetic acid; EGTA, ethylene glycol bis(β-aminoethyl ether)-*N,N,N',N'*-tetraacetic acid; PMSF, phenylmethanesulfonyl fluoride; α-[^{125}I]BGT, ^{125}I-labeled α-bungarotoxin; $NaDodSO_4$, sodium dodecyl sulfate; PPO, 2,5-diphenyloxazole; Temed, *N,N,N',N'*-tetramethylethylenediamine.

0006-2960/83/0422-3112$01.50/0